Compensating for migration stretch to improve the resolution of S-impedance and density inversion

Swetal Patel, Francis Oyebanji and Kurt J. Marfurt, The University of Oklahoma*

Summary

Zoeppritz's (1919) equations describe the partitioning of the P- and S-wave energy into transmitted and reflected components as a function of incident angle. The three-term approximation of the Zoeppritz's equations developed by Aki and Richards (1980) show that P-impedance (Z_P), S-impedance (Z_S) and density (ρ) can be estimated from the "PP" reflected waves as a function of incident angle. At near angles the PP reflection is only sensitive to changes in Z_P. At farther angles, the PP reflection is sensitive to changes in all three parameters, Z_P, Z_S and ρ. Because no converted waves are measured, the loss in resolution for inverted Z_S and ρ is due to migration stretch. Correction for migration stretch rather than conventional "stretch-mute" corrections provides three advantages: (1) preservation of far angles required for accurate ρ inversion, (2) improvement in the vertical resolution of Z_S and ρ volumes, and (3) preservation of far angles that provide greater leverage against multiples. We apply our workflow to data acquired in the Ft Worth Basin and retain incident angles up to 42° at the Barnett Shale target. Comparing the spectrum of Z_P, Z_S and ρ of the original gather and migration stretch compensated data, we find an insignificant improvement in Z_P, but a moderate to significant improvement in resolution of Z_S and ρ.

Methodology

The workflow is a modification of nonstretch NMO described by Zhang et al. (2013) and Mutlu and Marfurt (2015) who first applied reverse NMO to the migrated gathers. Here, we combined the reverse NMO and nonstretch NMO processes into one, significantly decreasing algorithmic complexity and increasing speed. If the vertical two-way travel time is given by T_0, then the travel time for the same flat reflector at source-receiver offset h for velocity v_{RMS} is given by

$$t(T_0, v_{\mathrm{RMS}}, h) = \left\{T_0^2 + \left[\frac{h}{v_{\mathrm{RMS}}(T_0)}\right]^2\right\}^{1/2}, \qquad (1)$$

where each trace is defined by a fixed offset, h. The change in two-way travel time t, as a function of the zero-offset travel time T_0 is simply

$$\frac{\partial t}{\partial T_0} = T_0\left\{T_0^2 + \left[\frac{h}{v_{RMS}(T_0)}\right]^2\right\}^{-1/2} < 1. \qquad (2)$$

Let's assume the earth is composed of a suite of J reflections at time t_j and reflection coefficient r_j. Let's also assume that the time-varying source wavelet can be represented by Morlet wavelets of the form $w(f_j,\phi_j)$. The seismic trace without the NMO correction is then

$$u(t) = \sum_{j=1}^{J} r_j \delta(t_j) w(f_j, \varphi_j). \qquad (3)$$

After an NMO correction, these wavelets are stretched which leads to low frequency in the far offset data. We can compensate this stretch by computing a wavelet compression factor, c, by mapping T_{0j} to t_j, from equation 1:

$$c_j = \frac{1}{T_{0j}}\left\{T_0^2 + \left[\frac{h}{v_{RMS}(T_0)}\right]^2\right\}^{1/2} > 1, \qquad (4)$$

which can then be used to scale the wavelets in equation 3 and generate the compensated trace

$$u_{\mathrm{comp}}(T_0) = \sum_{j=1}^{J} r_j \delta(T_{0j}) w(c_j f_j, \varphi_j). \qquad (5)$$

The input to the algorithms consists of migrated seismic gathers and either an RMS or migration velocity model (Figure 1). The output is a volume of gathers that have been compensated for migration stretch.

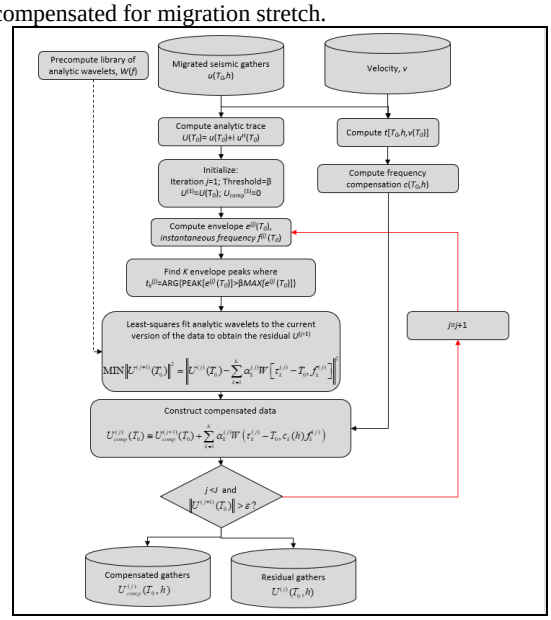

Figure 1. Algorithm flow chart for compensating migration stretch. The input to the algorithm is the migration velocity and the migrated seismic gathers.

Compensating for migration stretch to improve the resolution of S-impedance and density inversion

Figure 2a shows the input, unmuted CRP gather. Figure 2b shows the migration stretch compensated unmuted CRP gather. Figure 2c shows the data not modeled by the matching pursuit algorithm. Figure 2d shows the frequency compensation factor. The compensation factor increases with offset and decreases with depth, such that the far offset data of the shallower zone suffer from greater stretching. Note the higher resolution at the farther offsets at the Barnett Shale target at 1.1 s.

The original unmuted CRP gather, and unmuted stretch compensated CRP gather were conditioned for simultaneous inversion.

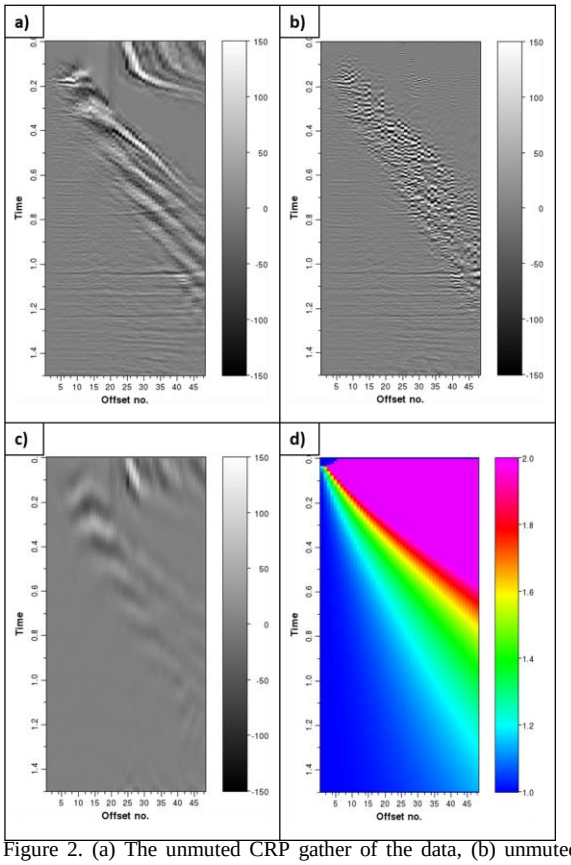

Figure 2. (a) The unmuted CRP gather of the data, (b) unmuted migration stretch compensated CRP gather, (c) unmodeled data and, (d) the frequency compensation factor. The farther the offset, the more frequency compensation factor.

Data Conditioning

In order to ascertain the value of the migration stretch, we applied the same suite of filters to the compensated and uncompensated gathers. First, we applied a seismic mute to remove high amplitude reverberations that overprint the shallow far-offset data. Then we applied parabolic Radon transform to discriminate between primaries and long period multiples. The gathers were transformed to velocity-stack domain, the low frequency noise is modelled and subsequently subtracted from the unmuted portion of the seismic gathers. Finally, we applied prestack structure-oriented filtering (Zhang et al., 2016, Sinha et al., 2017) using a Lower Upper Median (LUM) to suppress noise crosscutting the reflectors of interest.

Figure 3a and 3b shows a conditioned CRP gather before and after migration stretch compensation. Compensating for the migration stretch has considerably improved the resolution of the far offset data. Figure 4a and 4b shows that compensation for the migration stretch boosts high frequencies in the amplitude spectrum of the far angle stack (34°-42°) data. There is no compensation applied in the blue area of Figure 2d, such that the spectrum of the near offset data is unchanged.

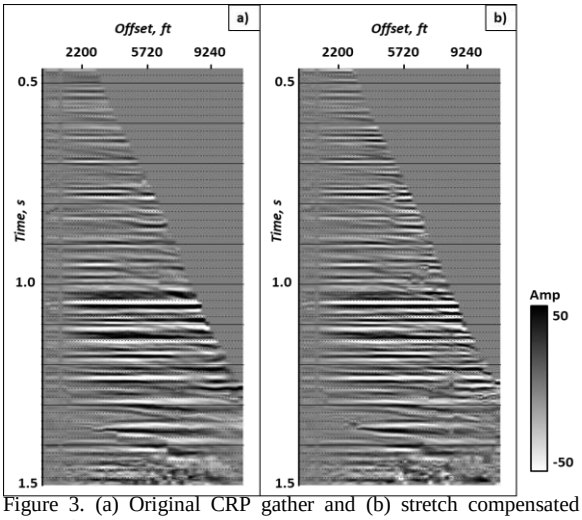

Figure 3. (a) Original CRP gather and (b) stretch compensated CRP after data conditioning. Both the data sets have been conditioned with same parameters. We observe an increase in resolution at far offset for stretch compensated data.

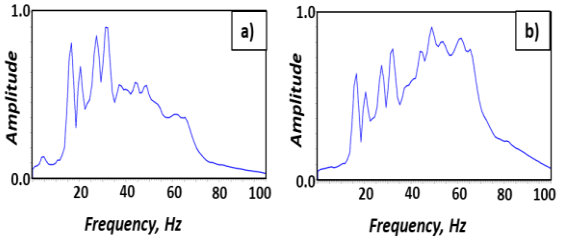

Figure 4. (a) Amplitude spectrum for far angle stack (34°-42°) for original CRP gather and (b) stretch compensated CRP gather. We observe a boost in the higher frequencies for the stretch compensated data.

Prestack simultaneous inversion

Figure 5 shows a cartoon of conventional "PP" seismic data acquisition. For a flat-layered geology and vertical incidence almost 100% of the near-offset reflected energy consists of PP reflections. Because the offset is small, the recorded seismic wavefield does not suffer from migration

stretch. At farther offsets (Figure 5b), the PP reflected event now suffers from migration stretch. The amplitudes of these farther offset PP reflections are sensitive not only the change in Z_P, but also of the change in Z_S and ρ (Figure 6). The gradient of the change of the PP reflection amplitude with angle is sensitive to the Z_S contrast across the boundary while the curvature near the critical angle is sensitive to ρ. It is this sensitivity of the PP reflection events to changes in all three parameters that allows us to invert for Z_S and density; unless we acquire multicomponent data, we do not measure the PS reflection events. While the PS reflection events will in general suffer from greater attenuation than the corresponding PP events, the lower resolution in Z_S and ρ compared to that of Z_P from PP reflected events is not due to attenuation but rather to the greater sensitivity of the Z_S inversion to the farther (stretched) offsets.

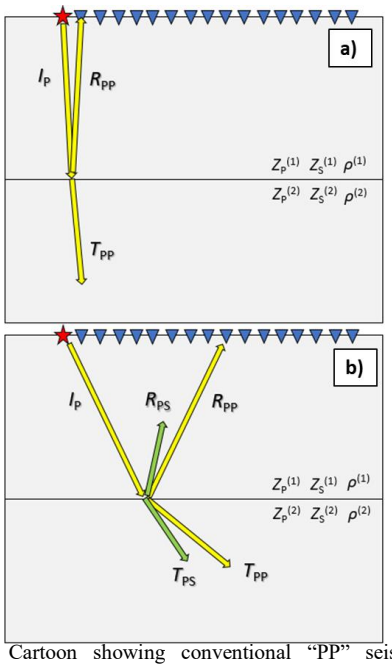

Figure 5. Cartoon showing conventional "PP" seismic data acquisition using vertical geophones (on land) or hydrophones (at sea). (a) At near-offsets the incident P wave generates only PP reflections and transmissions such that the PP reflection is sensitive only to changes in Z_P. (b) At farther offsets, the incident P wave generates both PP and PS reflections and transmissions, such that the PP reflection is sensitive to changes in Z_P, Z_S, and density.

Simultaneous inversion was carried out for original and stretch-compensated gathers to estimate Z_P, Z_S and ρ. The maximum usable incident angle of 42° at the Barnett Shale target allowed us to estimate ρ from inversion. Inversion of both data volumes was carried out exactly with the same parameters.

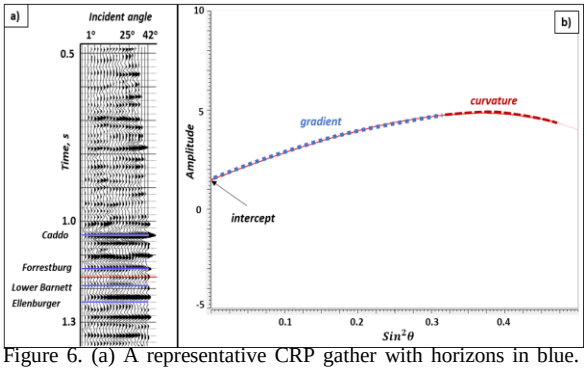

Figure 6. (a) A representative CRP gather with horizons in blue. (b) The AVO response of the event indicated by the red line in (a). The blue dashed line indicates the approximate AVO gradient. The red dashed line indicates the AVO curvature.

Figure 7a and 7b shows the Z_P estimated from simultaneous inversion of original prestack gather and migration stretch compensated gather respectively. A good match between the Z_{Plog} and $Z_{Pseismic}$ confirms the fidelity of the inversion. Because the near offsets that do not suffer from migration stretch are quite sensitive to changes in Z_P, there is little change in Z_P after stretch compensation (Figure 7).

Figure 8a-b shows Z_S and Figure 9a-b shows ρ estimated from simultaneous inversion of original prestack gathers and migration stretch compensated gathers respectively. A good match between the logs and inverted seismic volumes validates the fidelity in the inverted Zs and ρ volumes. Compensation for migration stretch produces a significant improvement in resolution of the Z_S and ρ in the shallow section and reduced improvements deeper as predicted by Figure 2d.

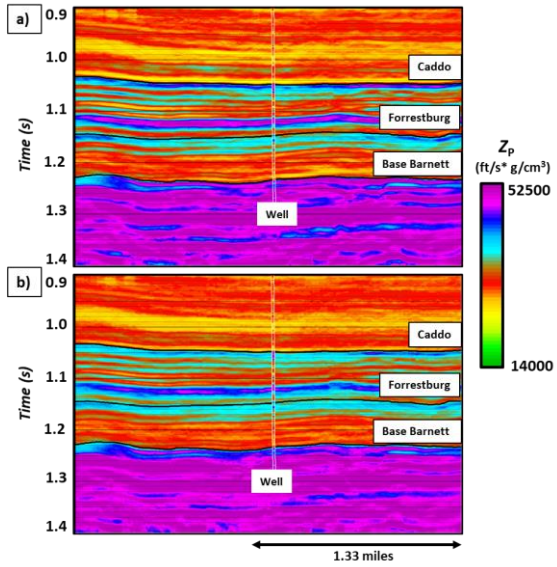

Figure 7. Z_P estimated from simultaneous inversion of a) original prestack gather and, b) migration stretch compensated prestack gather. We see insignificant improvement in resolution of Z_P from compensation of migration stretch

Compensating for migration stretch to improve the resolution of S-impedance and density inversion

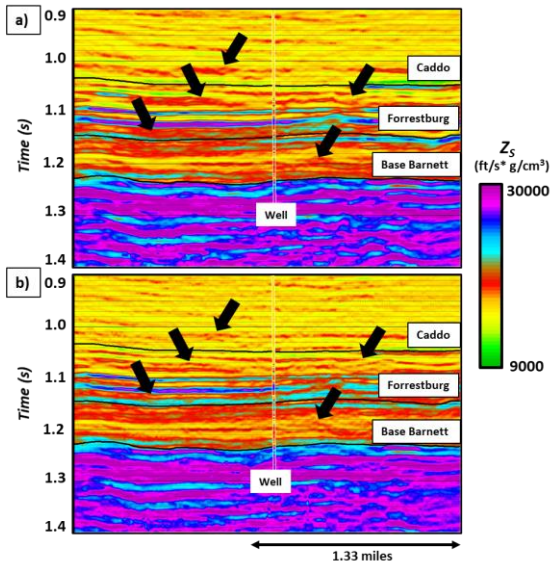

Figure 8. Z_S estimated from simultaneous inversion of (a) original prestack gather and, (b) migration stretch compensated prestack gather. The black arrows show areas of significant improvement in resolution of Z_S from compensation of migration stretch.

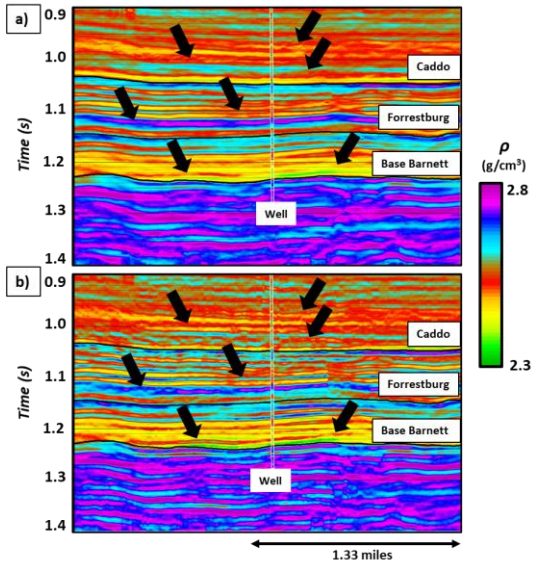

Figure 9. ρ estimated from simultaneous inversion of (a) original prestack gather and, (b) migration stretch compensated prestack gather. Black arrows indicate areas of significant improvement in resolution of ρ by compensating for migration stretch.

Conclusions

In principle, seismic reflections are represented by discrete spikes at reflector boundaries. These spikes are then convolved with the seismic wavelet to provide the seismic trace. Migration assumes each sample of the seismic trace is a potential reflection spike, leading to stretch of the imaged wavelets, which in turn leads to lower resolution for inverted S-impedance and density.

We use a matching pursuit algorithm to estimate the location of the reflection's spikes, fit wavelets to the data and then compensate for migration stretch. Comparison of the amplitude spectrum for the far angle stack (34°-42°) of the original gather and stretch-compensated gathers shows an increase in higher frequencies. Because P-impedance is heavily dependent on the zero angle reflected PP waves, there is an insignificant improvement in P-impedance resolution. In contrast, there is a significant improvement in resolution for Z_S and ρ in the shallow section and a moderate improvement in the deeper section.

Acknowledgments

Thanks to Pioneer Natural Resources Company for providing a license to their seismic data for use in research and education. Thanks to CGG Geosoftware for licenses to their Geoview inversion package. Finally, thanks to the sponsors of the AASPI consortium for their guidance and financial support.